Efficient Receiver Design for Uplink Cell-Free Massive MIMO With Hardware Impairments

Jiakang Zheng, Jiayi Zhang, *Member, IEEE*, Luming Zhang, Xiaodan Zhang, and Bo Ai, *Senior Member, IEEE*

***Abstract*—This paper investigates the effect of hardware impairments on the achievable performance of cell-free (CF) massive multiple-input multiple-output (MIMO) systems with four low-complexity receiver cooperation among the multiple antennas access points (APs), included large scale fading decoding (LSFD), simple LSFD, simple centralized decoding and small cell. Taking into account the joint hardware impairment (HI) effects brought by both APs and user equipments, we derive closed-form expressions for uplink spectral efficiency (SE) of CF massive MIMO systems. It is found that LSFD can achieve the largest SE. Furthermore, a novel hardware-quality scaling law is presented to reveal the relationship between the number of antennas and HI. Based on these results, we provide important insights into the practical impact of HI. For example, the impact of HI at the APs vanishes as the number of APs grows. Finally, numerical results validate our derived results.**

***Index Terms*—Hardware impairments, cell-free massive MIMO, receiver, spectral efficiency.**

I. Introduction

Cell-Free (CF) massive multiple-input multiple-output (MIMO) has been recently introduced as a useful and practical embodiment of the network MIMO concept, where a large number of geographically distributed access points (APs) coherently serve many user equipments (UEs) in the same time-frequency resource [1]. There are no cell boundary in CF massive MIMO. In contrast, in conventional distributed antenna system and cloud radio access network, the base station antennas are distributed within each cell, and these antennas only serve user terminals within that cell [2], [3]. Moreover, the ultra dense network presented in [4] and [5] increases the cell density to improve the capacity of systems, which suffers extremely inter-cell interference compared with CF massive MIMO. Recently, CF massive MIMO has received increasing research interests from academia. For instance, [6] presented the performance analysis of CF massive MIMO systems with low resolution analog-to-digital converters. The performance of CF massive MIMO systems with phase shifts over Rician was discussed in [7]. The authors in [8] use deep learning to obtain the channel estimation for CF massive MIMO. In this system, all benefits of massive MIMO can be reaped at a greater scale and it has been seen as an essential technique of the beyond-5G wireless systems [9], [10].

However, a majority of the existing works focuses on ideal hardware in both transceiver and receiver, which is not satisfied in practice. The reason is that the closer to ideal a hardware component is, the more challenging it is to implement, as it becomes bulkier, more expensive, and consumes more power [11], [12]. However, the effect of hardware impairments (HI) on CF massive MIMO has attracted little interest. Only in [13], a well-established HI model has been used to reveal the performance of both uplink and downlink CF massive MIMO. However, only low-performance maximum ratio receiver and simple independent Rayleigh fading channels have been considered in [13]. Recently, low-complexity and high-performance receiver cooperation are described and compared in [14], such as large-scale fading decoding (LSFD) and simple centralized decoding (S-CD).

Motivated by the above observations, we use the HI model in [11] to investigate the uplink performance of CF massive MIMO systems under low-complexity receiver cooperation. We derive closed-form expressions for the spectral efficiency (SE) of the non-ideal hardware CF massive MIMO systems with four kinds of receiver cooperation included LSFD, simple LSFD (S-LSFD), S-CD and small cell. We reveal how HI at the UEs and APs affect the SE of different receiver cooperation, and prove HI has larger impacts on the LSFD system. Finally, a useful hardware-quality scaling law is obtained to establish a precise relationship between the number of APs and the hardware quality factors.

Notation: Column vectors are represented by boldface lowercase letters, $\mathbf{x}$, and matrices are boldface uppercase letters, $\mathbf{X}$. We use superscripts $\mathbf{A}^{\mathrm{T}}$, $\mathbf{A}^{*}$ and $\mathbf{A}^{\mathrm{H}}$ to represent transpose, conjugate, and conjugate transpose, respectively. We use $\triangleq$ for definitions and $\mathrm{diag}(\mathbf{A}_1, \ldots, \mathbf{A}_n)$ for a block-diagonal matrix with the square matrices $\mathbf{A}_1, \ldots, \mathbf{A}_n$ on the diagonal. The nth element of $\mathbf{x}$ is denoted by $[\mathbf{x}]_n$, the mth row and nth column of $\mathbf{X}$ is denoted by $[\mathbf{X}]_{mn}$, $\odot$ denotes the Hadamard product. The expection value of $\mathbf{x}$ is denoted as $\mathbb{E}\{\mathbf{x}\}$. Finally, the multi-variate circularly symmetric complex Gaussian distribution with correlation matrix $\mathbf{R}$ is denoted as $\mathcal{N}_{\mathbb{C}}(\mathbf{0}, \mathbf{R})$, where $\mathbb{C}$ denotes complex set.

II. System Model

We consider a CF massive MIMO system consisting of L APs and K UEs. All APs are equipped with N antennas and each UE is equipped with a single antenna. The APs are connected to a CPU via fronthaul links. The independent and identically distributed (i.i.d.) Rayleigh fading channel[1] vector between AP l and UE k is $\mathbf{h}_{kl} \sim \mathcal{N}_{\mathbb{C}}(\mathbf{0}, \beta_{kl}\mathbf{I}_N)$, which is block fading with τ_c channel uses. Note that β_{kl} denotes the large-scale fading coefficient including pathloss and shadowing. In the uplink transmission, pilots occupy τ_p channel uses and $\tau_c - \tau_p$

[1]Note that the performance of CF massive MIMO systems mainly depends on the large-scale fading [1], [14]. The results for Rayleigh fading channels can be straightforwardly extended to other small-scale fading channels.

Manuscript received October 13, 2019; revised January 15, 2020; accepted February 17, 2020. Date of publication February 20, 2020; date of current version April 16, 2020. This work was supported in part by the National Key Research and Development Program under Grant 2016YFE0200900, in part by the Royal Society Newton Advanced Fellowship under Grant NA191006, in part by the State Key Lab of Rail Traffic Control and Safety under Grants RCS2018ZZ007 and RCS2019ZZ007, in part by the National Natural Science Foundation of China under Grants 61971027, U1834210, 61961130391, 61625106, and 61725101, in part by the Beijing Natural Science Foundation under Grants 4182049 and L171005, in part by the Open Research Fund of the State Key Laboratory of Integrated Services Networks under Grant ISN20-04, and in part by the Engineering Research Center of Mobile Communications, Ministry of Education under Grant CQUPT-MCT-201804, in part by Science and Technology Key Project of Guangdong Province China under Grant 2019B010157001, in part by the ZTE Corporation. The review of this article was coordinated by Prof. Y. Zhou. *(Corresponding authors: Jiayi Zhang; Xiaodan Zhang.)*

Jiakang Zheng and Jiayi Zhang are with the School of Electronics and Information Engineering, Beijing Jiaotong University, Beijing 100044, China, and also with the State Key Laboratory of Integrated Services Networks, Xidian University, Xi'an 710071, China (e-mail: jiayizhang@bjtu.edu.cn).

Luming Zhang is with the College of Computer Sciences, Zhejiang University, Hangzhou 310027, China (e-mail: zglumg@zju.edu.cn).

Xiaodan Zhang is with the School of Management, Shenzhen Institute of Information Technology, Shenzhen 518172, China (e-mail: zhangxd@sziit.edu.cn).

Bo Ai is with the State Key Laboratory of Rail Traffic Control and Safety, Beijing Jiaotong University, Beijing 100044, China, and also with the School of Information Engineering, Zhengzhou University, Zhengzhou 450001, China (e-mail: boai@bjtu.edu.cn).

Digital Object Identifier 10.1109/TVT.2020.2975354

channel uses for payload data. In addition, the HI at transceiver acts as a non-linear filter due to non-linear amplification, finite-resolution quantization, amplitude/phase imbalance in I/Q mixers, phase noise in LOs, and sampling jitter [15].

A. Pilot Transmission and Channel Estimation

The kth UE sends its pilot sequences $\mathbf{\Phi}_{t_k} \in \mathbb{C}^{\tau_p}$, which satisfies $\|\mathbf{\Phi}_{t_k}\| = \tau_p$. Our focus is a large network with $K > \tau_p$ so that more than one UE may use the same pilot. The pilot assigned to UE k is denoted by $t_k \in \{1, \ldots, \tau_p\}$ and other UEs that use the same pilot as UE k is denoted by $p_k \subset \{1, \ldots, K\}$. Therefore, the received signal $\mathbf{Z}_l \in \mathbb{C}^{N \times \tau_p}$ at AP l is

$$\mathbf{Z}_l = \sqrt{\kappa_r} \sum_{i=1}^{K} \mathbf{h}_{il} \left(\sqrt{\kappa_t p_i} \mathbf{\Phi}_{t_i}^{\mathrm{T}} + \left(\boldsymbol{\eta}_i^{\mathrm{UE}} \right)^{\mathrm{T}} \right) + \mathbf{G}_l^{\mathrm{AP}} + \mathbf{N}_l, \quad (1)$$

where $0 < \kappa_t \leqslant 1$ and $0 < \kappa_r \leqslant 1$ are the hardware quality factors of the transmitter and receiver, respectively [11]. $p_i \geqslant 0$ is the transmit power of UE i. In addition, $\mathbf{N}_l \in \mathbb{C}^{N \times \tau_p}$ is receiver noise whose elements are i.i.d. as $\mathcal{N}_{\mathbb{C}}(0, \sigma^2)$, and the transmitter distortion $\boldsymbol{\eta}_i^{\mathrm{UE}} \in \mathbb{C}^{\tau_p}$ is distributed as $\mathcal{N}_{\mathbb{C}}(\mathbf{0}_{\tau_p}, (1-\kappa_t) p_i \mathbf{I}_{\tau_p})$. For the receiver distortion matrix $\mathbf{G}_l^{\mathrm{AP}} \in \mathbb{C}^{N \times \tau_p}$, the columns are independently distributed as $\boldsymbol{\eta}_l^{\mathrm{AP}} \sim \mathcal{N}_{\mathbb{C}}(\mathbf{0}_N, \mathbf{D}_{l,\{\mathbf{h}\}})$, where

$$\mathbf{D}_{l,\{\mathbf{h}\}} \triangleq (1-\kappa_r) \sum_{i=1}^{K} p_i \mathrm{diag}\left(|[\mathbf{h}_{il}]_1|^2, \ldots, |[\mathbf{h}_{il}]_N|^2 \right). \quad (2)$$

To estimate $\mathbf{h}_{kl}$, we use the associated normalized pilot signal $\mathbf{\Phi}_{t_k} / \sqrt{\tau_p}$ and the received signal to obtain $\mathbf{z}_{t_k l} \triangleq \frac{1}{\sqrt{\tau_p}} \mathbf{Z}_l \mathbf{\Phi}_{t_k}^* \in \mathbb{C}^N$, which is given by

$$\begin{aligned} \mathbf{z}_{t_k l} = {} & \sqrt{\kappa_t \kappa_r p_k \tau_p} \mathbf{h}_{kl} + \sum_{i \in \mathcal{P}_k \setminus (k)} \sqrt{\kappa_t \kappa_r p_i \tau_p} \mathbf{h}_{il} \\ & + \sqrt{\frac{\kappa_r}{\tau_p}} \sum_{i=1}^{K} \mathbf{h}_{il} \left(\boldsymbol{\eta}_i^{\mathrm{UE}} \right)^{\mathrm{T}} \mathbf{\Phi}_{t_k}^* + \frac{\mathbf{G}_l^{\mathrm{AP}} \mathbf{\Phi}_{t_k}^*}{\sqrt{\tau_p}} + \frac{\mathbf{N}_l \mathbf{\Phi}_{t_k}^*}{\sqrt{\tau_p}}. \end{aligned} \quad (3)$$

With the help of well-known results from estimation theory [15, Lemma B.19], the linear minimum mean-square error (LMMSE) estimate of $\mathbf{h}_{kl}$ is

$$\hat{\mathbf{h}}_{kl} = \sqrt{\kappa_t \kappa_r p_k \tau_p} \boldsymbol{\beta}_{kl} \mathbf{I}_N \mathbf{\Psi}_{\tau_k l} \mathbf{z}_{t_k l}, \quad (4)$$

where

$$\mathbf{\Psi}_{\tau_k l} \triangleq \sum_{i \in \mathcal{P}_k} \kappa_t \kappa_r p_i \tau_p \beta_{il} \mathbf{I}_N + \sum_{i=1}^{K} p_i \left(1 - \kappa_t \kappa_r \right) \beta_{il} \mathbf{I}_N + \sigma^2 \mathbf{I}_N. \quad (5)$$

B. Uplink Data Transmission

During the uplink data transmission, the received complex baseband signal $\mathbf{y}_l$ at AP l is given by

$$\mathbf{y}_l = \sqrt{\kappa_r} \sum_{i=1}^{K} \mathbf{h}_{il} \left(\sqrt{\kappa_t} s_i + \eta_i^{\mathrm{UE}} \right) + \boldsymbol{\eta}_l^{\mathrm{AP}} + \mathbf{n}_l, \quad (6)$$

where $s_i \sim \mathcal{N}_{\mathbb{C}}(0, p_i)$ is the transmit signal from UE i with power p_i, and $\mathbf{n}_l$ is the independent receiver noise. In addition, η_i^{UE} and $\boldsymbol{\eta}_l^{\mathrm{AP}}$ are the hardware distortions at UE i and AP l.

III. Performance Analysis

A. Large-Scale Fading Decoding

The LSFD combining receiver allows each AP to do local channel estimation and to send it to the CPU for jointly detection. More specifically, AP l selects $\mathbf{v}_{kl}$ as the local combining receiver for UE k. Therefore, the local estimate[2] of s_k can be expressed as

$$\begin{aligned} \breve{s}_{kl} \triangleq {} & \mathbf{v}_{kl}^{\mathrm{H}} \mathbf{y}_l = \sqrt{\kappa_t \kappa_r} \mathbf{v}_{kl}^{\mathrm{H}} \mathbf{h}_{kl} s_k + \sqrt{\kappa_r} \mathbf{v}_{kl}^{\mathrm{H}} \mathbf{h}_{kl} \eta_k^{\mathrm{UE}} \\ & + \sqrt{\kappa_r} \sum_{i \neq k}^{K} \mathbf{v}_{kl}^{\mathrm{H}} \mathbf{h}_{il} \left(\sqrt{\kappa_t} s_i + \eta_i^{\mathrm{UE}} \right) + \mathbf{v}_{kl}^{\mathrm{H}} \boldsymbol{\eta}_l^{\mathrm{AP}} + \mathbf{v}_{kl}^{\mathrm{H}} \mathbf{n}_l. \end{aligned} \quad (7)$$

The CPU uses weights $\mathbf{a}_k$ to obtain $\hat{s}_k = \sum_{l=1}^{L} a_{kl}^* \breve{s}_{kl}$ as

$$\begin{aligned} \hat{s}_k = {} & \sqrt{\kappa_t \kappa_r} \left(\sum_{l=1}^{L} a_{kl}^* \mathbb{E}\left\{ \mathbf{v}_{kl}^{\mathrm{H}} \mathbf{h}_{kl} \right\} \right) s_k \\ & + \sqrt{\kappa_t \kappa_r} \left(\sum_{l=1}^{L} a_{kl}^* \left(\mathbf{v}_{kl}^{\mathrm{H}} \mathbf{h}_{kl} - \mathbb{E}\left\{ \mathbf{v}_{kl}^{\mathrm{H}} \mathbf{h}_{kl} \right\} \right) \right) s_k \\ & + \sqrt{\kappa_r} \sum_{i \neq k}^{K} \sum_{l=1}^{L} a_{kl}^* \mathbf{v}_{kl}^{\mathrm{H}} \mathbf{h}_{il} \left(\sqrt{\kappa_t} s_i + \eta_i^{\mathrm{UE}} \right) + \sum_{l=1}^{L} a_{kl}^* \mathbf{v}_{kl}^{\mathrm{H}} \boldsymbol{\eta}_l^{\mathrm{AP}} \\ & + \sqrt{\kappa_r} \left(\sum_{l=1}^{L} a_{kl}^* \mathbf{v}_{kl}^{\mathrm{H}} \mathbf{h}_{kl} \right) \eta_k^{\mathrm{UE}} + \sum_{l=1}^{L} a_{kl}^* \mathbf{v}_{kl}^{\mathrm{H}} \mathbf{n}_l. \end{aligned} \quad (8)$$

Theorem 1: Using MR combining with $\mathbf{v}_{kl} = \hat{\mathbf{h}}_{kl}$ and the use-and-then forget (UatF) bound,[3] the achievable SE of UE k is expressed as

$$\mathrm{SE}_k = (1 - \tau_p/\tau_c) \log_2 (1 + \mathrm{SINR}_k), \quad (9)$$

with SINR_k given in eq. (10) shown at the bottom of this page, where

$$\mathbf{a}_k \triangleq [a_{k1} \cdots a_{kL}]^{\mathrm{T}} \in \mathbb{C}^L, \quad (11)$$

$$\mathbf{b}_{kk} \triangleq [(\beta_{k1})^2 \Psi_{\tau_k 1} \cdots (\beta_{kL})^2 \Psi_{\tau_k L}]^{\mathrm{T}} \in \mathbb{C}^L, \quad (12)$$

$$\mathbf{\Lambda}_k \triangleq \mathrm{diag}\left((\beta_{k1})^2 \Psi_{\tau_k 1}, \cdots, (\beta_{kL})^2 \Psi_{\tau_k L} \right) \in \mathbb{C}^{L \times L}, \quad (13)$$

$$\mathbf{T}_{ki} \triangleq \mathrm{diag}\left(s_{ki1}, \ldots, s_{kiL} \right) \in \mathbb{C}^{L \times L}, \quad (14)$$

$$\mathbf{\Gamma}_{ki} \triangleq \mathrm{diag}\left(t_{ki1}, \ldots, t_{kiL} \right) \in \mathbb{C}^{L \times L}, \quad (15)$$

$$[\mathbf{H}_{ki}]_{ln} \triangleq \begin{cases} [\mathbf{c}_{ki} \mathbf{c}_{ki}^{\mathrm{H}}]_{ln}, (l \neq n) \\ 0, (l = n). \end{cases} \quad (16)$$

[2]Only keeping hardware qualities, the approximate SE expression can be written as $1/(1/(\kappa_r \kappa_t) + 1/\kappa_t + a)$, where a is a constant. It is clear that the SE significantly increases with the increasing values of κ_r and κ_t. In addition, κ_t has a greater influence on the uplink SE compared with κ_r.

[3]The UatF bound indicates the channel estimates are used for combining and then effectively "forgotten" before the signal detection [13, Theorem 4.4]. Therefore, only the first line of formula (8) is treated as the desired signal.

$$\begin{aligned} \mathrm{SINR}_k = {} & \frac{(\kappa_t \kappa_r p_k)^3 (\tau_p N)^2 \left| \mathbf{a}_k^{\mathrm{H}} \mathbf{b}_{kk} \right|^2}{\sum_{i=1}^{K} p_i \mathbf{a}_k^{\mathrm{H}} \bar{\mathbf{F}}_{ik} \mathbf{a}_k + \sum_{i \in p_k} (p_i)^2 \tau_p N \mathbf{a}_k^{\mathrm{H}} \bar{\mathbf{G}}_{ik} \mathbf{a}_k - (\kappa_t \kappa_r p_k)^3 (\tau_p N)^2 \left| \mathbf{a}_k^{\mathrm{H}} \mathbf{b}_{kk} \right|^2 + \sigma^2 p_k \kappa_t \kappa_r \tau_p N \mathbf{a}_k^{\mathrm{H}} \mathbf{\Lambda}_k \mathbf{a}_k} \\ \bar{\mathbf{F}}_{ik} \triangleq {} & p_k \kappa_t \kappa_r \tau_p N \mathbf{\Gamma}_{ki} + p_k p_i \kappa_t (1 - \kappa_t) (\kappa_r)^3 \tau_p N^2 \mathbf{H}_{ki} \\ \bar{\mathbf{G}}_{ik} \triangleq {} & p_k (\kappa_t \kappa_r)^2 \tau_p \left(1 + \kappa_r (N-1) \right) \mathbf{T}_{ki} + p_k \tau_p N \kappa_r (\kappa_t \kappa_r)^2 \mathbf{H}_{ki} \end{aligned} \quad (10)$$

In addition, s_{kil}, t_{kil} and $\mathbf{c}_{ki}$ are expressed as

$$s_{kil} \triangleq (\beta_{kl})^2(\beta_{il})^2\left(\Psi_{\tau_k l}\right)^2, \tag{17}$$

$$t_{kil} \triangleq (\beta_{kl})^2\beta_{il}\Psi_{\tau_k l} + p_i(\beta_{kl})^2(\beta_{il})^2\left(\Psi_{\tau_k l}\right)^2 \times \left(1-\kappa_t\kappa_r+(1-\kappa_t)(\kappa_r)^2(N-1)\right), \tag{18}$$

$$\mathbf{c}_{ki} \triangleq [\beta_{k1}\beta_{i1}\Psi_{\tau_k 1}\cdots\beta_{kL}\beta_{iL}\Psi_{\tau_k L}]^{\mathrm{T}} \in \mathbb{C}^L. \tag{19}$$

Note that $\Psi_{\tau_k l}$ is a scalar expressed as

$$\Psi_{\tau_k l} \triangleq \mathrm{tr}\left(\mathbf{\Psi}_{\tau_k l}\right)/N = 1\Big/\left(\sum_{i\in\mathcal{P}_k}\kappa_t\kappa_r p_i\tau_p\beta_{il} + \sum_{i=1}^{K} p_i(1-\kappa_t\kappa_r)\beta_{il} + \sigma^2\right). \tag{20}$$

Proof: Please refer to Appendix A.

Note that (10) is a generalized Rayleigh quotient with respect to $\mathbf{a}_k$. With the help of [15, Lemma B.10], the effective SINR for UE k is maximized by

$$\mathbf{a}_k = \left(\sum_{i=1}^{K} p_i\bar{\mathbf{F}}_{ik} + \sum_{i\in p_k}(p_i)^2\tau_p N\bar{\mathbf{G}}_{ik} - (\kappa_t\kappa_r p_k)^3(\tau_p N)^2\mathbf{b}_{kk}\mathbf{b}_{kk}^{\mathrm{H}} + \sigma^2 p_k\kappa_t\kappa_r\tau_p N\mathbf{\Lambda}_k\right)^{-1}\mathbf{b}_{kk}, \tag{21}$$

which leads to the maximum SINR value

$$\mathrm{SINR}_k^{\mathrm{LSFD}} = (\kappa_t\kappa_r p_k)^3(\tau_p N)^2\mathbf{b}_{kk}^{\mathrm{H}}\left(\sum_{i=1}^{K} p_i\bar{\mathbf{F}}_{ik} + \sum_{i\in p_k} p_i{}^2\tau_p N\bar{\mathbf{G}}_{ik} - (\kappa_t\kappa_r p_k)^3(\tau_p N)^2\mathbf{b}_{kk}\mathbf{b}_{kk}^{\mathrm{H}} + \sigma^2 p_k\kappa_t\kappa_r\tau_p N\mathbf{\Lambda}_k\right)^{-1}\mathbf{b}_{kk}. \tag{22}$$

Remark 1: In order to reduce the complexity of LSFD, we propose S-LSFD with the simple weights $a_{kl} = \beta_{kl}/\sum_{k=1}^{K}\beta_{kl}$. However, it causes performance loss compared with LSFD as shown in numerical results.

Remark 2: According to [14], a large number of statistical parameters that grows quadratically with L and K is required for LSFD, which have a heavy loading effect. Therefore, S-CD is employed with the simple weights $\mathbf{a}_k = [1/L\ldots 1/L]^{\mathrm{T}}$.

Theorem 2: Considering $\kappa_t = \kappa_{t0}/L^{\varepsilon_t}$, $\kappa_r = \kappa_{r0}/L^{\varepsilon_r}$, for constants $\kappa_{t0}, \kappa_{r0} \in (0,1]$, where ε_t, ε_r denote scaling exponents in transceiver. Therefore, only $\varepsilon_t = 0$ and $0 < \varepsilon_r < 1/2$ can lead to $\mathrm{SE}_k \to \log_2(1+\mathrm{SINR}_k^{\infty})$ as $L\to\infty$, where

$$\mathrm{SINR}_k^{\infty} = \frac{(p_k)^2\tau_p N}{\sum_{i=1}^{K}\frac{(p_i)^2(1-\kappa_t)N}{(\kappa_t)^2} + \sum_{i\in p_k}\frac{(p_i)^2\tau_p N}{\kappa_t} - (p_k)^2\tau_p N}. \tag{23}$$

TABLE I
NUMBER OF COMPLEX SCALARS FROM THE APS TO THE CPU VIA THE FRONTHAUL AND THE COMPUTATIONAL COMPLEXITY OF WEIGHT $\mathbf{a}_k$

Method	Fronthaul requirement	Complexity analysis
LSFD	$(\tau_c-\tau_p)KL$	K^2L^2
S-LSFD	$(\tau_c-\tau_p)KL$	K^2
S-CD	$(\tau_c-\tau_p)KL$	—
Small cell	—	—

Proof: It follows similar steps in [15, Corollary 6.8].

Theorem 2 proves that we can decrease κ_r roughly as $1/\sqrt{L}$ and still achieve the same SE limit by increasing the number of APs L. However, the convergence speed to the SE limit is much slower if the hardware quality gradually reduces.

B. Small Cell

For small cell networks, an achievable SE of UE k is the maximum one among all APs [15, Sec. 6] in eq. (24) shown at the bottom of this page, where

$$\bar{F}_{ikl} \triangleq 1 + p_i\beta_{il}\Psi_{\tau_k l}\left(1-\kappa_t\kappa_r+(1-\kappa_t)(\kappa_r)^2(N-1)\right)/(\kappa_t\kappa_r)^2,$$

$$\bar{G} \triangleq 1+\kappa_r(N-1)/N\kappa_t\kappa_r. \tag{25}$$

Following similar steps in [14], we provide complexity analysis and fronthaul requirement of four different receiver cooperation as shown in Table I. It is clear that LSFD, S-LSFD and S-CD have the same fronthaul requirement. However, the complexity of LSFD increases with L since it requires the $L\times L$ matrix inverse to derive $\mathbf{a}_k$ in (21).

IV. NUMERICAL RESULTS AND DISCUSSION

In this section, we quantitatively study the performance of CF Massive MIMO with HI under different parameters and receiver cooperation. According to [1] and [14], we assume that the L APs and K UEs are independently and uniformly distributed within a square of size $1\times 1\ \mathrm{km}^2$. The large-scale fading coefficient β_{kl} models the path loss and shadow fading, according to $\beta_{kl} = \mathrm{PL}_{mk}\cdot 10^{(\sigma_{\mathrm{sh}}z_{mk})/10}$, where PL_{mk} represents the path loss, and $10^{(\sigma_{\mathrm{sh}}z_{mk})/10}$ represents the shadow fading with the standard deviation $\sigma_{\mathrm{sh}} = 8$ dB, and $z_{mk}\sim\mathcal{N}(0,1)$. In addition, $p_i = 100$ mW and $\tau_c = 200$ are considered.

We first compare the performance of the considered system with four different receiver cooperation in Fig. 1. It is clear that the SE increases with the increasing of the hardware qualities κ_t and κ_r, which also can be easily observed in (7). Moreover, it is interesting to see from Table II that LSFD has the maximum median and 95%-likely (i.e., where the vertical axis is 0.05) performance loss when the hardware qualities reduce from 1 to 0.9. The reason is that the LSFD requires more knowledge of statistical parameters, which is easier to be affected. In addition, the correctness of analytical results is verified by the simulation results.

Fig. 2 shows the cumulative distribution of uplink average SE with different values of the quality factors in the transmitter and receiver. It is clear that the parameter κ_t has a greater influence on the uplink average SE compared with the parameter κ_r. For example, the uplink average SE reduces by 8.67% when only κ_r decreases from 1 to 0.9.

$$\mathrm{SINR}_{kl} = \frac{(p_k\beta_{kl})^2\tau_p\Psi_{\tau_k l}N}{\sum_{i=1}^{K}p_i\beta_{il}\bar{F}_{ikl} + \sum_{i\in p_k}(p_i\beta_{il})^2\tau_p\Psi_{\tau_k l}N\bar{G} - (p_k\beta_{kl})^2\tau_p\Psi_{\tau_k l}N + \frac{\sigma^2}{(\kappa_t\kappa_r)^2}} \tag{24}$$

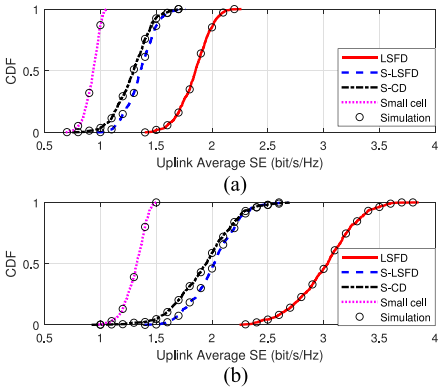

Fig. 1. Uplink average SE with four different receiver cooperation ($L = 100, K = 10, N = 2, \tau_p = 5$). (a) $\kappa_t = \kappa_r = 0.9$; (b) $\kappa_t = \kappa_r = 1$.

TABLE II
PERFORMANCE LOSS OF DIFFERENT RECEIVER COOPERATION ($\kappa_t = \kappa_r = \kappa$)

Method	Median SE			95%-likely SE		
	κ=1	κ=0.9	Loss	κ=1	κ=0.9	Loss
LSFD	3.04	1.85	39.14%	2.52	1.59	36.90%
S-LSFD	2.02	1.36	32.67%	1.66	1.13	31.93%
S-CD	1.95	1.29	33.85%	1.51	1.02	32.45%
Small cell	1.32	0.94	28.79%	1.13	0.80	29.20%

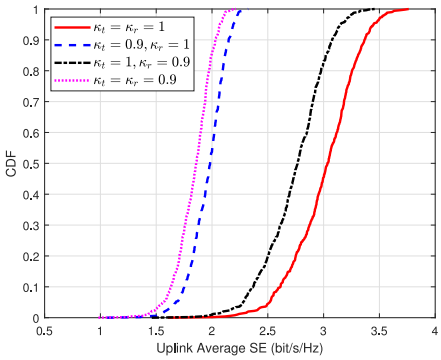

Fig. 2. Uplink average SE with LSFD for different values of κ_t and κ_r ($L = 100, K = 10, N = 2, \tau_p = 5$).

However, only reducing κ_t from 1 to 0.9 can causes 36.46% SE loss, which is close to the SE loss for the case of $\kappa_t = \kappa_r = 0.9$.

The uplink sum SE is shown in Fig. 3, as a function of the number of APs. It is clear that the SE increases with the number of APs L. In addition, Fig. 3 validates the hardware-quality scaling law that the uplink sum SE converges to a non-zero limit, when $\varepsilon_t = 0$, $0 \leqslant \varepsilon_r < 1/2$. Therefore, we can obtain the conclusion that the reducing hardware quality can be compensated by adding more antennas or APs when $\varepsilon_t = 0, \varepsilon_r < 1/2$. Note that sum SE denotes the sum of SE for all UEs. Here we use it to indicate the overall performance.

V. CONCLUSION

In this correspondence, we derived novel and exact closed-form expressions for SE of the CF massive MIMO system with HI and four low-complexity receiver cooperation. Moreover, a useful hardware-quality scaling law is obtained. The obtained results show that the hardware distortion has a larger impact on the performance of LSFD

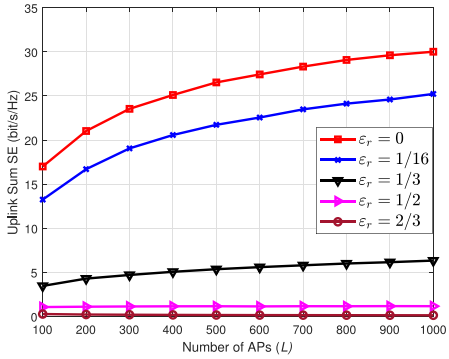

Fig. 3. Uplink sum SE with LSFD against the number of APs L for different values of ε_r ($K = 5, N = 2, \tau_p = 3, \kappa_t = 0.997, \kappa_{r0} = 0.997$).

compared to other three receiver cooperation. In addition, the influence of HI at UEs is greater than the one at APs. Furthermore, the detrimental effect of HI at the APs vanishes when the number of APs grows large.

APPENDIX A
PROOF OF THEOREM 1

Following a similar approach in [15, Theorem 6.2], the desired signal and the interference in (8) are derived as

$$P_{\text{desired}} = \kappa_t \kappa_r p_k \left| \sum_{l=1}^{L} a_{kl}^* \mathbb{E}\left\{ \mathbf{v}_{kl}^{\mathrm{H}} \mathbf{h}_{kl} \right\} \right|^2, \tag{26}$$

$$\begin{aligned} P_{\text{interference}} = \mathbb{E}\left\{ |V_{\text{interference}}|^2 \right\} &= \kappa_r \sum_{i=1}^{K} \mathbb{E}\left\{ \left| \sum_{l=1}^{L} a_{kl}^* \mathbf{v}_{kl}^{\mathrm{H}} \mathbf{h}_{il} \right|^2 \right\} \\ &\times \left(\kappa_t \mathbb{E}\left\{ |s_i|^2 \right\} + \mathbb{E}\left\{ |\eta_i^{\mathrm{UE}}|^2 \right\} \right) \\ &- \kappa_t \kappa_r \left| \sum_{l=1}^{L} a_{kl}^* \mathbb{E}\left\{ \mathbf{v}_{kl}^{\mathrm{H}} \mathbf{h}_{kl} \right\} \right|^2 \mathbb{E}\left\{ |s_k|^2 \right\} \\ &+ \mathbb{E}\left\{ \left| \sum_{l=1}^{L} a_{kl}^* \mathbf{v}_{kl}^{\mathrm{H}} \boldsymbol{\eta}_l^{\mathrm{AP}} \right|^2 \right\} + \mathbb{E}\left\{ \left| \sum_{l=1}^{L} a_{kl}^* \mathbf{v}_{kl}^{\mathrm{H}} \mathbf{n}_l \right|^2 \right\}. \end{aligned} \tag{27}$$

Note that there is $\mathbb{E}\{|\sqrt{\kappa_t} s_i + \eta_i^{\mathrm{UE}}|^2\} = \mathbb{E}\{|s_i|^2\} = p_i$ in the considered HI model. Using [7, Eq. (91)], we have

$$\begin{aligned} \mathbb{E}\left\{ \left| \sum_{l=1}^{L} a_{kl}^* \mathbf{v}_{kl}^{\mathrm{H}} \mathbf{h}_{il} \right|^2 \right\} &= \sum_{l=1}^{L} |a_{kl}^*|^2 \mathbb{E}\left\{ \left| \mathbf{v}_{kl}^{\mathrm{H}} \mathbf{h}_{il} \right|^2 \right\} \\ &+ \sum_{l=1}^{L} \sum_{n \neq l}^{L} a_{kl} a_{kn}^* \mathbb{E}\left\{ \left(\mathbf{v}_{kl}^{\mathrm{H}} \mathbf{h}_{il} \right)^* \left(\mathbf{v}_{kn}^{\mathrm{H}} \mathbf{h}_{in} \right) \right\}. \end{aligned} \tag{28}$$

In addition, the distribution of the receiver distortion can be expressed as [15, Eq. (6.12)]

$$\boldsymbol{\eta}_l^{\mathrm{AP}} = \sqrt{1 - \kappa_r} \sum_{i=1}^{K} \sqrt{p_i} \mathbf{h}_{il} \odot \bar{\boldsymbol{\eta}}_{il}^{\mathrm{AP}}, \tag{29}$$

where $\bar{\boldsymbol{\eta}}_{il}^{\mathrm{AP}} \sim \mathcal{N}_{\mathbb{C}}(\mathbf{0}_N, \mathbf{I}_N)$ is an independent random variable. Therefore, we have

$$\mathbb{E}\left\{ \left| \sum_{l=1}^{L} a_{kl}^* \mathbf{v}_{kl}^{\mathrm{H}} \boldsymbol{\eta}_l^{\mathrm{AP}} \right|^2 \right\} = \sum_{l=1}^{L} |a_{kl}^*|^2 \mathbb{E}\left\{ \left| \mathbf{v}_{kl}^{\mathrm{H}} \boldsymbol{\eta}_l^{\mathrm{AP}} \right|^2 \right\}$$

$$= \sum_{l=1}^{L} |a_{kl}^*|^2 (1-\kappa_r) \sum_{i=1}^{K} p_i \mathbb{E}\left\{ \left| \mathbf{v}_{kl}^{\mathrm{H}} \left(\mathbf{h}_{il} \odot \bar{\boldsymbol{\eta}}_{il}^{\mathrm{AP}} \right) \right|^2 \right\}$$

$$= \sum_{l=1}^{L} |a_{kl}^*|^2 (1-\kappa_r) \sum_{i=1}^{K} p_i \mathbb{E}\left\{ \left\| \mathbf{v}_{kl} \odot \mathbf{h}_{il} \right\|^2 \right\}. \quad (30)$$

Furthermore, the noise term in (27) can be written as

$$\mathbb{E}\left\{ \left| \sum_{l=1}^{L} a_{kl}^* \mathbf{v}_{kl}^{\mathrm{H}} \mathbf{n}_l \right|^2 \right\} = \sigma^2 \sum_{l=1}^{L} |a_{kl}^*|^2 \mathbb{E}\left\{ \left\| \mathbf{v}_{kl} \right\|^2 \right\}. \quad (31)$$

With the help of [15, Corollary 6.3], we can obtain

$$\mathbb{E}\left\{ \mathbf{v}_{kl}^{\mathrm{H}} \mathbf{h}_{kl} \right\} = \mathbb{E}\left\{ \left\| \mathbf{v}_{kl} \right\|^2 \right\} = p_k \kappa_t \kappa_r (\beta_{kl})^2 \tau_p \Psi_{\tau_k l} N, \quad (32)$$

$$\mathbb{E}\left\{ \left| \mathbf{v}_{kl}^{\mathrm{H}} \mathbf{h}_{il} \right|^2 \right\} = p_k \kappa_t \kappa_r (\beta_{kl})^2 \beta_{il} \tau_p \Psi_{\tau_k l} N$$
$$+ p_k p_i \kappa_t \kappa_r (\beta_{kl})^2 (\beta_{il})^2 \tau_p \left(\Psi_{\tau_k l} \right)^2 N \left(1 - \kappa_r + (1-\kappa_t) \kappa_r N \right)$$
$$+ \begin{cases} p_k p_i (\kappa_t \kappa_r)^2 (\beta_{kl})^2 (\beta_{il})^2 \left(\tau_p \Psi_{\tau_k l} N \right)^2, (i \in p_k) \\ 0, (i \notin p_k) \end{cases}, \quad (33)$$

$$\mathbb{E}\left\{ \left\| \mathbf{v}_{kl} \odot \mathbf{h}_{il} \right\|^2 \right\} = p_k \kappa_t \kappa_r (\beta_{kl})^2 \beta_{il} \tau_p \Psi_{\tau_k l} N$$
$$+ p_k p_i \kappa_t \kappa_r (\beta_{kl})^2 (\beta_{il})^2 \tau_p \left(\Psi_{\tau_k l} \right)^2 N \left(1 - \kappa_t \kappa_r \right)$$
$$+ \begin{cases} p_k p_i (\kappa_t \kappa_r)^2 (\beta_{kl})^2 (\beta_{il})^2 \left(\tau_p \Psi_{\tau_k l} \right)^2 N, (i \in p_k) \\ 0, (i \notin p_k) \end{cases}, \quad (34)$$

$$\mathbb{E}\left\{ \left(\mathbf{v}_{kl}^{\mathrm{H}} \mathbf{h}_{il} \right)^* \left(\mathbf{v}_{kn}^{\mathrm{H}} \mathbf{h}_{in} \right) \right\}$$
$$= p_k p_i \kappa_t \left(1 - \kappa_t \right) \kappa_r^2 \tau_p N^2 \beta_{kl} \beta_{il} \Psi_{\tau_k l} \beta_{kn} \beta_{in} \Psi_{\tau_k n}$$
$$+ \begin{cases} p_k p_i (\kappa_t \kappa_r \tau_p N)^2 \beta_{kl} \beta_{il} \Psi_{\tau_k l} \beta_{kn} \beta_{in} \Psi_{\tau_k n}, (i \in p_k) \\ 0, (i \notin p_k) \end{cases}. \quad (35)$$

The proof is finished by substituting (32–35) into (26–31).

REFERENCES

[1] H. Q. Ngo, A. Ashikhmin, Y. Hong, E. G. Larsson, and T. L. Marzetta, "Cell-free massive MIMO versus small cells," *IEEE Trans. Wireless Commun.*, vol. 16, no. 3, pp. 1834–1850, Mar. 2017.

[2] G. N. Kamga, M. Xia, and S. Aïssa, "Spectral-efficiency analysis of massive MIMO systems in centralized and distributed schemes," *IEEE Trans. Commun.*, vol. 64, no. 5, pp. 1930–1941, May 2016.

[3] X. Wang *et al.*, "Virtualized cloud radio access network for 5G transport," *IEEE Commun. Mag.*, vol. 55, no. 9, pp. 202–209, Sep. 2017.

[4] L. Liu, Y. Zhou, W. Zhuang, J. Yuan, and L. Tian, "Tractable coverage analysis for hexagonal macrocell-based heterogeneous UDNs with adaptive interference-aware CoMP," *IEEE Trans. Wireless Commun.*, vol. 18, no. 1, pp. 503–517, Jan. 2018.

[5] L. Liu, Y. Zhou, V. Garcia, L. Tian, and J. Shi, "Load aware joint CoMP clustering and inter-cell resource scheduling in heterogeneous ultra dense cellular networks," *IEEE Trans. Veh. Technol.*, vol. 67, no. 3, pp. 2741–2755, Mar. 2017.

[6] X. Hu, C. Zhong, X. Chen, W. Xu, H. Lin, and Z. Zhang, "Cell-free massive MIMO systems with low resolution ADCs," *IEEE Trans. Commun.*, vol. 67, no. 10, pp. 6844–6857, Oct. 2019.

[7] Ö. Özdogan, E. Björnson, and J. Zhang, "Performance of cell-free massive MIMO with Rician fading and phase shifts," *IEEE Trans. Wireless Commun.*, vol. 18, no. 11, pp. 5299–5315, Nov. 2019.

[8] Y. Jin, J. Zhang, S. Jin, and B. Ai, "Channel estimation for cell-free mmwave massive MIMO through deep learning," *IEEE Trans. Veh. Technol.*, vol. 68, no. 10, pp. 10 325–10 329, Oct. 2019.

[9] J. Zhang, E. Björnson, M. Matthaiou, D. W. K. Ng, H. Yang, and D. J. Love, "Multiple antenna technologies for beyond 5G," 2019, *arXiv:1910.00092*.

[10] J. Zhang, S. Chen, Y. Lin, J. Zheng, B. Ai, and L. Hanzo, "Cell-free massive MIMO: A new next-generation paradigm," *IEEE Access*, vol. 7, pp. 99 878–99 888, 2019.

[11] E. Björnson, J. Hoydis, M. Kountouris, and M. Debbah, "Massive MIMO systems with non-ideal hardware: Energy efficiency, estimation, and capacity limits," *IEEE Trans. Inf. Theory*, vol. 60, no. 11, pp. 7112–7139, Nov. 2014.

[12] Q. Zhang, T. Q. Quek, and S. Jin, "Scaling analysis for massive MIMO systems with hardware impairments in Rician fading," *IEEE Trans. Wireless Commun.*, vol. 17, no. 7, pp. 4536–4549, Jul. 2018.

[13] J. Zhang, Y. Wei, E. Björnson, Y. Han, and S. Jin, "Performance analysis and power control of cell-free massive MIMO systems with hardware impairments," *IEEE Access*, vol. 6, pp. 55 302–55 314, 2018.

[14] E. Björnson and L. Sanguinetti, "Making cell-free massive MIMO competitive with MMSE processing and centralized implementation," *IEEE Trans. Wireless Commun.*, vol. 19, no. 1, pp. 77–90, Jan. 2020.

[15] E. Björnson, J. Hoydis, and L. Sanguinetti, "Massive MIMO networks: Spectral, energy, and hardware efficiency," *Found. Trends Signal Process.*, vol. 11, no. 3–4, pp. 154–655, 2017.